



Research Article

Numerical analysis of spiral tube heat exchanger circulated with zinc oxide nanofluids

K. P. V. Krishna VARMA¹, Kavati VENKATESWARLU^{2,*}, Teku KALYANI¹, S. HEMALATHA¹,
P. Vijaya KUMAR¹

¹Department of Mechanical Engineering, Raghu Engineering College, Andhra Pradesh, 531162, India

²Department of Mechanical Engineering, University of Namibia, School of Engineering and the Built Environment, JEDS Campus, Ongwediva, 3624, Namibia

ARTICLE INFO

Article history

Received: 18 July 2024

Revised: 17 October 2024

Accepted: 22 October 2024

Keywords:

CFD; Heat Transfer Coefficient;
Helical Coil Heat Exchanger;
Reynolds Number; ZnO
Nanofluids

ABSTRACT

Helical tube heat exchangers differ from ordinary heat exchangers in that they have special qualities that enhance heat transmission since the fluid flows from straight to coiled channels as curved streams instead of linear ones, leading to the increased momentum and heat transmission rates. However, there is still scope for research on improving heat transfer characteristics for a helical coil heat exchanger with conjugate heat transfer employing various configurations of internal longitudinal fins. Thus, in this work, numerical study was conducted to explore the flow behaviour and thermal performance of water-ZnO nanofluids (nanofluid) in a spiral tube heat exchanger. The mass flow rate (\dot{m}) of the water-ZnO nanofluids was varied from 0.025 kg/s to 0.125 kg/s, while the mass flow rate of the hot fluid (water) was maintained constant at 0.0091 kg/s. The concentrations of the nanofluid in water used were 1%, 2%, and 3%. Simulations in three dimensions were analysed for the turbulent stream regime, and governing equations for the turbulent stream were solved using the k-epsilon ($k-\epsilon$) for Reynolds numbers ranging from 4000 to 12000. The temperature, velocity and pressure contours were analysed with respect to the variation in the concentration and flow rate of the ZnO nanofluids. Finally, the results confirmed that by applying ZnO nanofluids, the heat transfer coefficient as well as the friction factor increased by 43% and 1.12 times respectively when compared with the plain tube.

Cite this article as: Varma KPVK, Venkateswarlu K, Kalyani T, Hemalatha S, Kumar PV. Numerical analysis of spiral tube heat exchanger circulated with zinc oxide nanofluids. J Ther Eng 2025;11(2):377–389.

INTRODUCTION

Heat exchangers have been essential parts for more than a century in air conditioning, refrigeration systems and many industrial processes that need to be heated, cooled,

or undergone isothermal operations [1]. Heat transfer enhancement in a heat exchanger is drawing a wider attention, especially from an industrial community, since it reduces the heat transfer area for a particular heat exchanger.

*Corresponding author.

*E-mail address: vakavati@unam.na, chaitu9903@gmail.com

This paper was recommended for publication in revised form by
Editor-in-Chief Ahmet Selim Dalkılıç



The trend of heat exchanger devices in the future will face challenges in terms of weight and size reduction, increased heat transmission efficiency, and cost reduction [2]. The primary benefits of increasing the heat exchanger performance can be the reduced cost and material, and energy savings in the heat exchange process [3]. Heat transfer enhancement techniques can be categorized into passive, active and compound methods. One of the best methods of improvement is passive method, which improves the heat transfer while requiring no outside power [4, 5].

Helical coil heat exchangers (HCHEs) are devices in which the heat is transferred from hot fluid to cold fluid through a separating cylindrical wall. Because of their small diameters, these helical coil heat exchangers are mainly suited for high-temperature and high-pressure applications. HCHEs are available at a low cost comparatively, however, the space occupancy of these heat exchangers is high compared to other heat exchangers. HCHEs are used in applications like solar water heaters, nuclear reactors, heat recovery systems and automotive systems. Since double pipe heat exchangers (DPHE) can establish a maximum temperature difference between the shell side and tube side fluids, they are widely utilized in industrial and engineering applications such as heat ventilation and air conditioning (HVAC), heat recovery, refrigeration and chemical reactors, etc. [6].

Many studies and articles in reputable scientific and engineering journals claim that when heat exchangers use nanofluids as working fluids, their heat transfer capabilities significantly improve. Nanoparticles are typically composed of metals, metal oxides, metal carbides, or carbon nanotubes. Because of these well-known qualities of nanoparticles, adding them to the fluids is a useful method of enhancing heat transfer. They have thermal conductivities that are higher than those of typical fluids due to their enormous surface area, which increases heat transport [7]. Numerous benefits of using nanofluids in systems have been noted, including increased heat conductivity and decreased pressure drop. However, the degree to which heat transfer is improved depends on the quantity of nanoparticles added to the base fluid [8]. These fluids also have special qualities that make them suitable for use in a number of other applications, including grinding, microchips, domestic refrigerators, hybrid power engines, and pharmaceutical processes [9]. A rise in thermal conductivity results in a rise in performance of heat transfer. Actually, the decrease in the thickness of the thermal boundary layer as a result of the random mobility of nanoparticles in the base fluid might make significant contributions to this kind of heat transfer enhancement [10-12]. For instance, adding 0.3 volume % of copper nanoparticles to ethylene glycol boosts its thermal conductivity by 40% [13], while adding 1 volume % of carbon nanotubes increases a synthetic poly(α -olefin) oil's thermal conductivity by 150% [14]. However, the difficulties brought about by the financial constraints resulting from the high cost of traditional nanoparticles like gold (80

USD/g), diamond (35 USD/g), and silver (6 USD/g), prevent their commercialization [15].

Several researchers studied both experimentally and numerically the addition of nanoparticles to the base fluid and their effect on heat transfer performance of heat exchangers. Kola et al. [16] showed that the combination of the cut's radius of twisted tapes and angle of cut has a substantial impact on heat transfer coefficient (HTC) and friction factor of a DPHE. Within the examined range, the ideal parameters to achieve increased HTC and decreased friction factor include mass flow rate of 0.05 kg/s, cut radius of 5.464 mm, and cut angle of 45°. Yang et al. [17] examined the heat transmission coefficient nanoparticles of graphite disseminated in liquid for laminar stream in a horizontal pipe heat exchanger. Investigations are carried out on the effects of the heat transmission coefficient on the Reynolds number, volume fraction, temperature, type of nanoparticles, and kind of base fluid. Their findings demonstrated that the heat transmission coefficient raised as the Re and particle concentration increased. In another study, Bahmani et al. [18] examined heat transmission and turbulent - stream for H₂O / Al₂O₃, nanofluid in a parallel and counter flow DPHEs. The results show that the Nusselt number and thermal efficiency enhanced by 32.70% and 30.0% respectively. However, the finding from the investigation reported that the increase in nanoparticle volume fraction increases the outlet temperature of fluid and wall temperatures. On the other hand, the heat exchanger's thermal efficiency enhancement slope eventually approaches a constant value as the Reynolds number increases. In parallel flow, this tendency is more pronounced, for this reason, they conclusively reported to use counterflow heat exchangers at higher Reynolds numbers. In another finding, Hasan [19] suggested that by applying an Al₂O₃ / H₂O nanofluid, especially at a low Reynolds number, there was a decrement observed in temperature of the outer wall pipe, compared with pure H₂O.

Attia et al. [20] showed that by combining Al₂O₃ nanoparticles with the salt water inside the solar still, the efficiency of solar still was enhanced by 127% and 174% respectively with the addition of 1g/L Al₂O₃ and 2g/L Al₂O₃. Pulagam et al. [21] showed that the Nusselt number was unaffected by concentration variations of Al₂O₃, indicating that the fluid's thermal conductivity and hydraulic diameter were the only factors influencing the heat transfer coefficient. The pressure drop rose as the chevron angle, pitch, and concentration increased, while the friction factor remained constant over a range of concentrations.

Kola et al. [22] optimised the variables such as the flow rate (m) of nanofluids, the cut radius, and the cut angle in a DPHE by inserting twisted tapes with different cross sections to maximise heat transmission and reduce the friction factor. They reported that the cut radius and cut angle are more effective than the flow rate and volume loading. Palanisamy and Mukesh Kumar [23] used multi-walled carbon nanotubes (MWCNTs)/water nanofluids in a cone helically coiled

tube heat exchanger and explored the heat transmission and pressure drop. At 0.1%, 0.3%, and 0.5% volume concentration of the nanofluids, the experimental Nu number is 28.0%, 52.0%, and 68.0% higher than H₂O. The pressure drop is also observed at 16.0%, 30.0%, and 42.0% higher at 0.1%, 0.3%, and 0.5%, respectively, which shows that using nanofluids resulted in a higher pressure drop than water.

Mukesh Kumar and Chandrasekar [24] investigated the heat transmission and pressure drop of the DHCHE using MWCNT/H₂O, nanofluids at 0.2%, 0.4%, and 0.6% volume concentrations and analysed the findings using computational software by setting the laminar stream conditions with the Dean number ranging from 1300 to 2200. The experimental and simulated results confirmed improved heat transmission rate, pressure drop with increased volume concentration. The Nu and pressure drop of the experimental and CFD data have a standard deviation of 8.5% and 7.2%, respectively. Onyiriuka et al. [25] investigated a mango bark nanofluid's turbulent flow heat transmission characteristic in a DPHE. The nanoparticle size of 100 nm is considered for this study. The observation reported an increment in the Nu by 68% and 45% for the Reynolds number values of 5000 and 13000 respectively, and improvement in the heat transmission coefficient of nanofluid was observed as twice that of base fluid. Gupta et al. [26] performed CFD analysis on a concentric tube heat exchanger to determine the total heat transmission coefficient, heat transmission rate, and pressure loss characteristics using Al₂O₃/H₂O, nanofluids with a Reynolds number range between 2000 – 10000. The result from the analysis reported that the overall-heat transmission coefficient, heat transmission rate, and pressure loss increased with increasing volume concentration of Al₂O₃/H₂O, nanofluids. The experimental analysis confirmed that the nanofluids with 0.5%, 1.5%, and 2.5% volume concentrations enhanced 7.2 %, 13.58 %, and 21.38 % in overall heat transmission coefficient, and improvement in heat transmission rates of 6.11%, 12.45%, and 17.27% was observed at 0.5%, 1.5%, and 2.5% volume concentrations respectively with a penalty of pressure loss.

Arya et al. [27] prepared MgO-ethylene glycol (EG) nanofluids at a weight concentration of 0.1%, 0.2%, and 0.3% to assess the heat transmission coefficient as well as friction factor of a DPHE. The flow rate and mass concentration of nanoparticles are the input operating parameters, and the output variables, like heat transmission coefficient and pressure drop, were investigated experimentally. The analysis exhibited that the heat transmission coefficient of the heat exchanger intensified by 27% with a nanofluid wt.% of 0.3 compared with the EG. However, increased pressure drops and friction factor of 35% and 32%, respectively are reported. The investigation confirmed that the friction factor decreased with an increased Reynolds number. Rafi et al. [28] reviewed the research works the researchers performed on optimising helical coil tube heat exchangers (HCHE) using Taguchi methods, Artificial Neural Network(ANN), Genetic Algorithm(GA), and

Multi-Objective Genetic Algorithm. Their studies reported that ANN and GA methods have proved suitable for modelling and optimising the HCTHE. Kannadhasan et al. [29] evaluated the heat transmission rate of CuO nanoparticles in a DPHE using CFD. The CuO nanoparticles at varying mass concentrations of 0.1 %, 0.2 %, and 0.3 % were organised and tested in the heat exchanger. The findings demonstrated that the CuO nanoparticle significantly lowered the cold-H₂O inlet temperature, and the heat transmission rate increased considerably from 183 to 3488 kW. The influence of a lower concentration of CuO nanoparticles was less significant than a higher concentration of suspended particles, as demonstrated by simulation findings.

Inyang and Uwa [30] reviewed the usefulness of the HCHE. Their study discussed various shapes of helical coils and their influence on the performance and effectiveness of heat exchanger's and compared them with straight tube heat exchangers. The study suggested that the helical coil heat exchanger augments heat transmission performance and effectiveness compared to straight tubes. The research findings from the study testified that the appropriate fluids must be selected to achieve high efficiency in HCHEs. Armstrong et al. [31] conducted studies with the hybrid nanofluid consisting of silver nitrate with molarities of 0.03 M, 0.06 M, and 0.09 M in graphene oxide (Ag-GO hybrid nanofluid), operating at a Reynolds number of 1,451 and a flow rate of 47 g/s. They found the improvements in heat transfer coefficient, Nusselt number, and thermal performance index as 62.9%, 33.55%, and 1.29%, respectively. Thus, the studies based on experimental and numerical analyses performed by several researchers revealed that varying the volume concentration and Reynolds number for different nanofluids with the output parameters such as decrement in pressure drop, Nusselt number, and Dean number were tested and compared. Using varying pressure and velocity during the inflow, Nashine and Singh [32] examined the heat transfer, friction factor, pressure differential, and Nusselt number of a helical coil tube for various values of Dean number [ratio of coil diameter (D) to tube diameter (d)]. According to their findings, the helical tube's heat transfer rises with a higher Dean number. In laminar flow, pressure increases have no influence on heat transfer, but in turbulent flow, they can have a negative impact. Finally, studies conducted by several researchers have reported that enhanced heat transmission augmentation is observed.

The majority of the analyses were carried out with either keeping wall temperature or heat flux constant, as with the boundary conditions. However, numerical research on improving heat transmission characteristics for a helical coil heat exchanger with conjugate heat transfer employing various configurations of internal longitudinal fins is still lacking. Moreover, the research on HCHE is primarily focused on nanofluids such as Al₂O₃, CuO and TiO₂, however, numerical analysis of helical coil heat exchanger circulated with ZnO nanofluids is rarely discussed. Also, the curvature of the tubes induces centrifugal forces, which in

turn result in the development of the secondary flow, leading to the enhancement in heat transfer. In addition to this, the increase in the thermal conductivity of the base fluid with the ZnO nanofluids enhances the rate of heat transfer. Therefore, in this current work, the focus is to analyse the effect of the curvature of the tubes and the effect of the helical coil along with the circulation of ZnO nanofluids in the helical coil heat exchanger. In this regard, the focus is on comparing the heat transfer characteristics of the helical coil heat exchanger using different concentration of the ZnO nanofluids for a counter flow helical coil heat exchanger. The numerical simulation using CFD and the heat transmission characteristics, such as heat transmission rate and coefficient, were analysed.

CFD MODELLING OF SPIRAL TUBE HEAT EXCHANGER

Physical Model

Since the nanoparticles are mixed in the water and are sent into the tubes of heat exchanger, the fluid is considered as a homogeneous mixture. Hence the fluid is modelled as single-phase fluid. The model used for the flow is

single phase model and the heat transfer is considered as the conjugate heat transfer. Simulations were carried out on HCHE with water - ZnO nanofluids of different concentrations. The HCHE is schematically shown in Figure 1. The thickness of the tube is 3 mm. The inner and outer diameters of the tube are 15 mm and 18 mm respectively. The distribution of the temperature of the hot and cold fluids are shown in the temperature contours of the helical coil heat exchanger circulated with the water and ZnO nanofluids. Initially, a 3D-HCHE is modelled with one pipe placed concentrically inside the other larger diameter pipe. A 3D numerical model of the HCHE is illustrated in Figure 2. The modelling of the HCHE is carried out using the procedure outlined in the below sections. Initially, select the first sketch in the x-y plane; then, extrude it up to a length of 1600 mm. Next, extrude another sketch up to 1600 mm, and the operation changes from adding material to adding frozen. A procedure similar to that of extruding sketch3 and sketch4 up to 1600 mm length in the z-direction is repeated, and the operation from adding material to adding frozen is changed. By extruding the entire body and switching the operation by adding material to add frozen, four (4) different parts and four (4) bodies, the details of HCHE are displayed in Table 1.

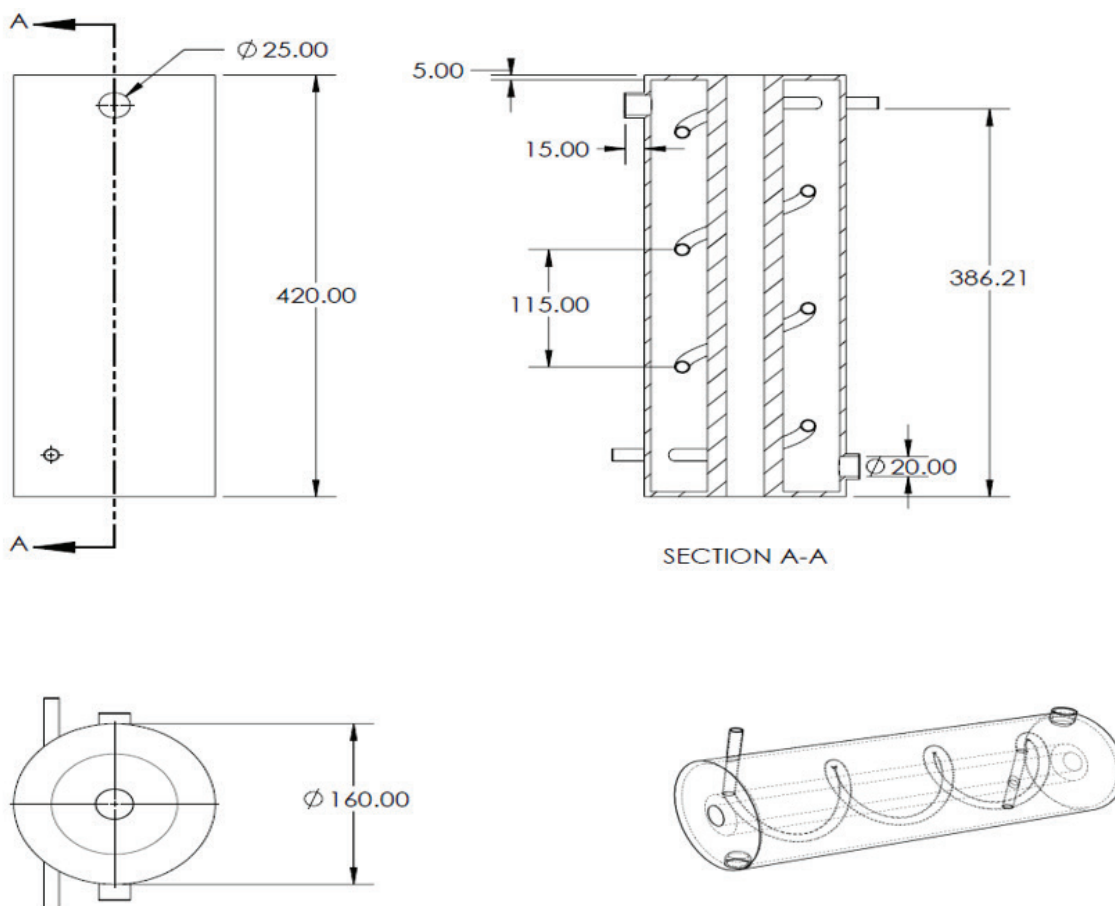


Figure 1. Helical coil heat exchanger.

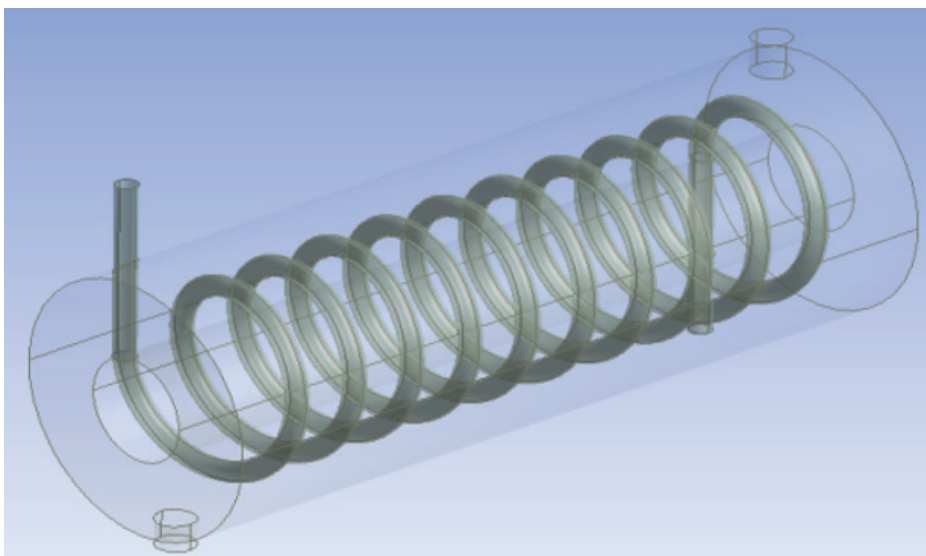


Figure 2. Geometry for meshing of helical coil heat exchanger.

Table 1. Particulars of the spiral tube heat exchanger

Part of the model	Type of state
Helical fluid	Fluid
Helical pipe	Solid
Outer fluid	Fluid
Outer pipe	Solid

Computational Grid Generation

The mesh used is comparatively a coarser and has mixed cells (tetra and hexahedral cells) with boundary faces that are triangular and quadrilateral as shown in Figure 3. But every attempt is made to use tetrahedral cells as much as possible, with the goal of minimizing diffusion by carefully defining the mesh’s structure, especially in the vicinity of the wall region. However, a fine mesh is produced after wards. For this thin mesh, the boundaries and areas of high pressure and temperature gradients are finely mesh. Turbulence modelling for the near-wall treatment depends mainly on the value of y^+ is indicated as a non-dimensional distance, commonly employed to predict the mesh’s fineness or coarseness for a specific flow pattern and ascertain the ideal cell size to domain walls. In addition, the y^+ value near the wall is constrained due to the turbulence model wall laws. As an illustration, the typical k-epsilon model requires a wall y^+ value between 300 and 100. However, to get higher values of y^+ , a greater flow velocity near the wall requires a reduction in grid size. Table 2 presents the values for different wall treatments, and Table 3 presents the mesh details employed in this experiment.

Mesh quality is an important parameter, which shows that the worst cells will have an orthogonal quality, which

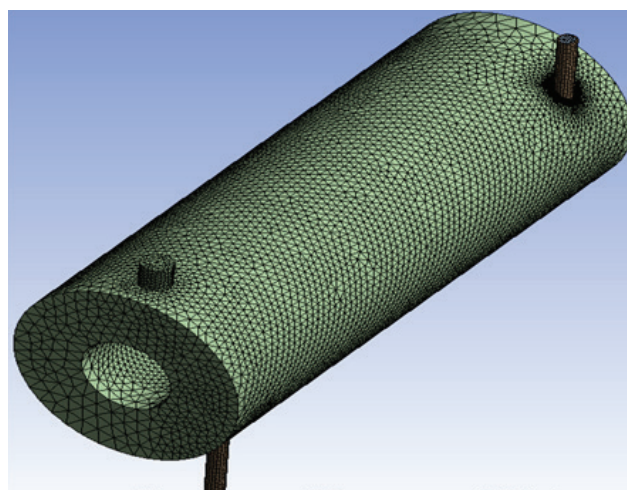


Figure 3. Closed view of mesh parts of helical coil heat exchanger.

will be close to 0. But the best cells possess orthogonal quality which is very close to 1. The mesh attributes like orthogonal quality and the skewness are assessed. Minimum and maximum orthogonal qualities achieved were 0.38 and 1.0 restrictively while the maximum skewness achieved is 0.5. The numerical model is meshed using the coarse mesh initially with 500000 elements and is modified to medium mesh with the elements of the mesh being increased to 1000000. Finally, the model is meshed with fine meshing containing the mesh elements of 2000000. First, there is a noticeable difference in the outlet temperature. The variation in the outlet temperature became stable when the mesh was taken into consideration. It was discovered that the outlet temperature variation was less than one suggesting that the outcomes are not influenced by the mesh that

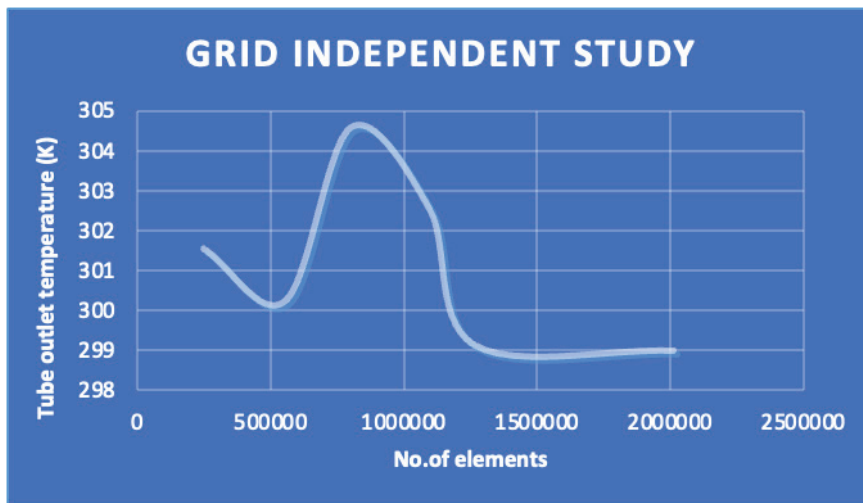


Figure 4. Grid independence study.

Table 2. y^+ values for different wall treatments

Wall treatment method	Recommended y^+ value	Used y^+ value at tube wall
Standard wall function	$30 < y^+ < 400$	$y^+ < 5$
Non equilibrium wall function	$30 < y^+ < 100$	$y^+ < 5$
Low Reynolds number model	$y^+ = 1$	$y^+ < 1$

Table 3. Details of the mesh

Feature	Type and range
Relevance centre	Fine meshing
Smoothing	High
Size	0.7479 mm to 74.797 mm
Number of nodes	1045694
Number of elements	703592

was used. As such, fine mesh is taken into account in this research. Grid independence study is illustrated in Figure 4.

Governing Equations

Navier Stokes equations are used for solving the equations. Continuity, momentum and energy equations [33] are considered for solving the numerical problem. k -epsilon (k - ϵ), turbulence model is used for analyzing the turbulence in the tubes of the heat exchanger. The conservation equations which control the core equation generally used in analytical fluid dynamics and CFD, are given below.

For a two-dimensional (2-D) incompressible fluid flow, the continuity equation (mass conservation) is written as

$$\frac{\partial u}{\partial x} + \frac{\partial v}{\partial y} = 0 \quad (1)$$

For a two-dimensional (2-D) incompressible fluid flow, the Navier-Stokes equation (momentum conservation) is given below

$$\frac{\partial u}{\partial t} + u \frac{\partial u}{\partial x} + v \frac{\partial u}{\partial y} = -\frac{\partial p}{\partial x} + \mu \left(\frac{\partial^2 u}{\partial x^2} + \frac{\partial^2 u}{\partial y^2} \right) \quad (2)$$

For a two-dimensional (2-D) incompressible fluid flow, the energy conservation equation is given as

$$\frac{\partial T}{\partial t} + u \frac{\partial T}{\partial x} + v \frac{\partial T}{\partial y} = \frac{k}{\rho c_p} \left(\frac{\partial^2 T}{\partial x^2} + \frac{\partial^2 T}{\partial y^2} \right) \quad (3)$$

The generalised heat diffusion equation of conduction is given as

$$\rho c \frac{\partial T}{\partial t} = k \nabla^2 T + \dot{q} \quad (4)$$

The heat transmission coefficient (h) for convection based on Newton's law of cooling, given as

$$q = \bar{h}(T_s - T_\infty) = \bar{h} \Delta T \quad (5)$$

where, T_s is the temperature over the surface, T_∞ is the temperature of the fluid and \bar{h} is the average heat transfer coefficient ($W/m^2 \cdot K$).

It is well recognized that there are two forms of convection: forced convection, which occurs when fluid flow is created by external devices like fans and blowers, and natural convection, which occurs when fluid moves because of buoyancy.

$$h \propto \Delta T^{\frac{1}{4}} \tag{6}$$

$$h \propto \Delta T^{\frac{1}{3}} \tag{7}$$

where $h = \text{constant}$

However, a generalised heat (Q) equation for conduction to represent the influence of fluid motion, assuming fluid to be incompressible, constant properties, negligible shear heating and neglecting changes in kinetic as well as potential energy is given as

$$\rho c \frac{\partial T}{\partial t} + \mathbf{u} \cdot \nabla T = k \nabla^2 T + \dot{q} \tag{8}$$

Also, the distribution of temperature in the boundary layer is solved to calculate ‘h’ using Fourier’s law given as

$$h = \frac{q}{T_w - T_\infty} = \frac{k}{T_w - T_\infty} \left. \frac{\partial T}{\partial y} \right|_{y=0} \tag{9}$$

The fluid flow as well as the problems of heat transfer can be tightly integrated over the term of convection in the equation of energy when the features rely on temperature.

The Analogy Between Heat Transmission and Momentum

In forced convection analysis, we are primarily interested in the determination of quantities such as local friction coefficient, C_{fx} and Nusselt number. It is desirable to have a relation between C_{fx} and Nusselt number, so that we can calculate one while other is available. Such relationships are developed on the basis of similarity between momentum and heat transfer in boundary layers, known as Reynolds analogy. For a given geometry, the friction coefficient can be expressed in terms of Reynolds number and x (dimensionless space variable) [34] given as

$$C_{f,x} \frac{Re_L}{2} = Nu_x \quad (Pr = 1) \tag{10}$$

Therefore, Eq. (10) is a significant similarity because it makes it possible to calculate the heat transmission coefficient of fluids with a Prandtl number, $Pr \approx 1$, using the friction coefficient, which is more easily measured. Similarly, another alternative way to express the Reynolds analogy is mentioned in Eq. (11).

$$\frac{C_{f,x}}{2} = St_x \quad (Pr = 1) \tag{11}$$

where $St_x = \frac{h}{\rho c_p V} = \frac{Nu}{Re_L Pr}$ (12)

is the Stanton number, another dimensionless heat transfer coefficient.

In order to solve the four unknown (u, v, p, and t) parameters, the incompressible flows involving temperature differences that lead to density differences and buoyancy-driven flows require the use of four equations they are: continuity, two halves of the N-S equation, and one energy equation.

The unknowns u, v, and P are determined using the continuity and Navier-Stokes equations. Further, these unknown calculated values ‘u’ and ‘v’ are substituted in the energy equation to obtain an unknown temperature; hence, the procedure is termed as coupling the energy equation with the continuity and momentum equations.

Boundary Conditions

Model requirements serve as the foundation for establishing boundary conditions. The intake condition is specified as the flow rate (\dot{m}), while the exit condition is determined by pressure. The heat exchanger model is designed as a counter-flow and parallel-flow model with two (2) tubes comprising two inlets and two outlets. A no-slip criterion was established for every wall, and each has its own specification and corresponding boundary conditions. Further, each wall is set to zero heat flux, except for the tube walls, and the details of all the boundary conditions are represented in Table 4. The outside diameter of the tube is 18 mm and the inside diameter is 15 mm. The hot fluid is flowing through the outside diameter and the cold fluid is flowing through the inside diameter. The outer and inside tube diameters are depicted in Figure 1. The temperature distribution across the inner and outer diameters of the tube are depicted in the temperature contours of the helical tube and helical tube circulated with the ZnO nanofluids. The named selections of the boundary conditions are depicted in Figure 5. ‘A’ represents the inlet of the cold fluid, ‘C’ denotes the outlet of the cold fluid. While ‘D’ represents the inlet of the hot fluid and ‘B’ denotes the outlet of the hot fluid.

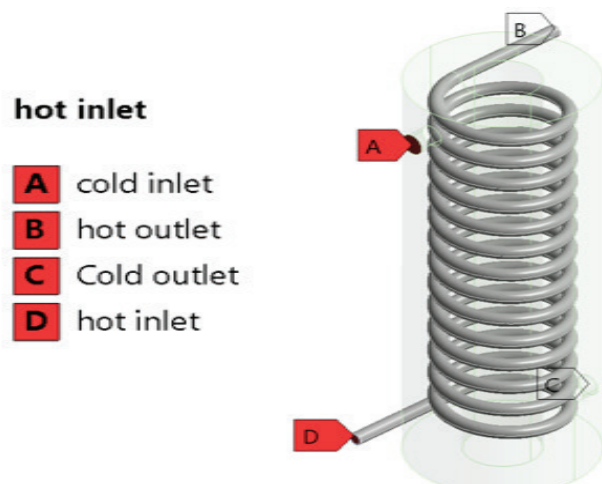


Figure 5. Named selections of the boundary conditions.

Table 4. Boundary conditions for parallel and counter flow heat exchangers

Inlet condition	Boundary condition type	Mass flow rate at inlet (kg/s)	Turbulent intensity (%)	Hydraulic diameter(mm)	Temperature (K)
Hot inlet	Mass flow inlet	0.0091	4.6	20	353
Hot outlet	Pressure outlet	-	4.6	-	-
Cold inlet	Mass flow inlet	0.025-0.125	3.6	35	288
Cold outlet	Pressure outlet	-	3.6	-	-

RESULTS AND DISCUSSION

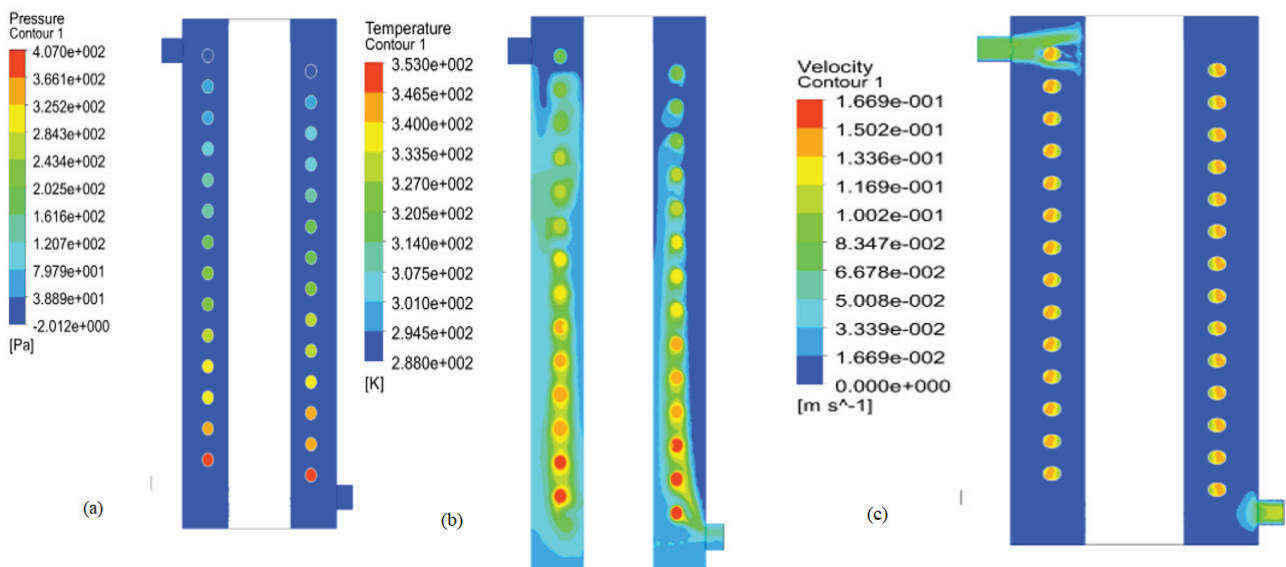
Contours of Plain Tube

The contours shown in Figure 6 (a-c) depict the temperature (T), pressure (p), and velocity (v) distribution along the heat exchanger for the plain tube at a \dot{m} of 0.175 kg/s. These contours represent the distribution of the hot and cold fluids through the helical coil HE with water circulating in the heat exchanger tubes. In addition, the maximum pressure distribution of the heat exchanger arises at 407 Pa on the tube side and 38.84 Pa on the shell side, as depicted in Figure 6 (a). Further, the heat exchanger temperature distribution showed a maximum temperature of 352.9 K, as illustrated in Figure 6 (b); however, the pictorial representation illustrated that the temperature on the tube side was reduced from 353 K to 318.14 K since the heat transmission between the hot and cold fluids was observed. Similarly, Figure 6 (c) represents the velocity distribution in heat exchanger through a variation in the velocity (v) of 0.169 m/s on the tube side.

ZnO Contours

Case 1: Simulation of HCHE for ZnO with volume loading of 1% and flow rate, $\dot{m} = 0.075$ kg/s

The distribution of hot and cold fluid through HCHE with a 1.0% ZnO mixture is illustrated in Figure 7 (a-c), and the heat exchanger pressure distribution represents the occurrence of a maximum pressure of 407 Pa at the tube side and 3.816 Pa at the shell side is shown in Figure 7(a). This depicts that there is a reduction in the pressure which is due to the circulation of the ZnO nanofluids in the tubes of the heat exchanger. This drop is attributed to the relative movement of the ZnO nanoparticles with respect to the wall and the intermixing of the nanoparticles in the tubes of the heat exchanger. There arises a wall friction as well as internal friction between the nanoparticles due to the bulk flow mixing of the nanoparticles in the fluid. This results in the drop in pressure in the HCHE. Also, the temperature distribution of the HE illustrates a maximum temperature of 352.9 K, which is recorded in Figure 7(b). However, it is noticed from the figure that the temperature on the tube side was reduced to 298.257 K from 353 K due to the heat

**Figure 6.** (a-c) Contours of water as a cold side fluid for a mass flow rate of 0.175 kg/s.

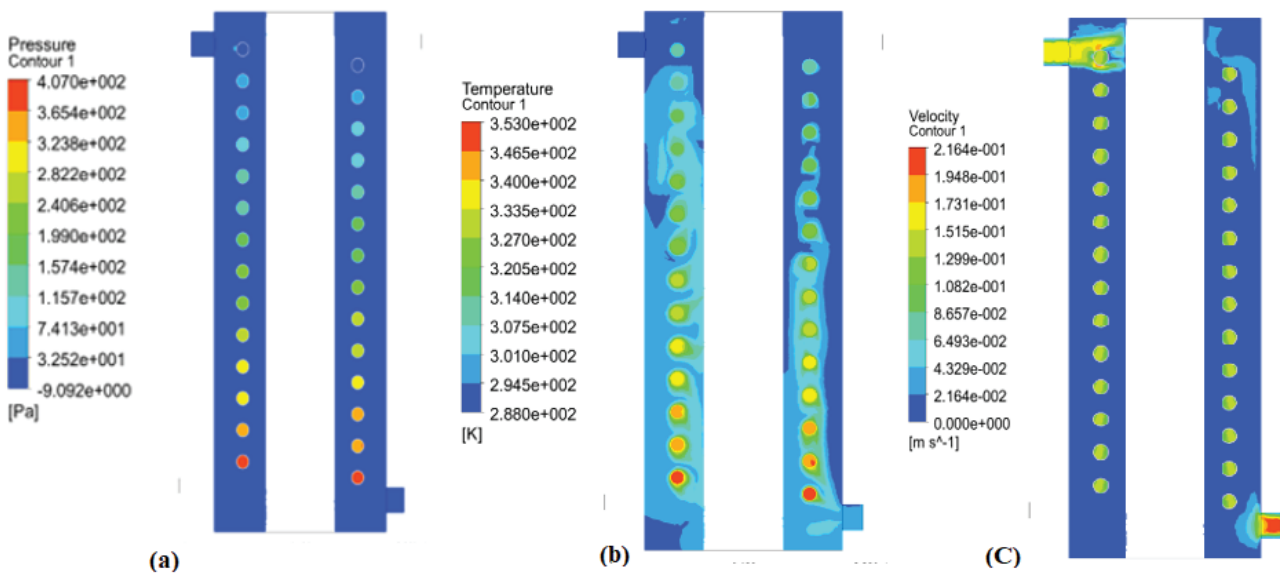


Figure 7. Contours of 1% ZnO as a cold side fluid for a mass flow rate of 0.175 kg/s for ZnO with volume fraction of 2% and $\dot{m}=0.075$ kg/s.

transmission effect between hot and cold fluid. The reason for this is attributed to the increase in the heat transmission due to the circulation of the 1% ZnO nanofluids in the tubes of the heat exchanger. This is in turn attributed to the increase in the thermal conductivity of the base fluid. In addition, the velocity distribution of the heat exchanger is one of the effective parameters, and it was noticed that the maximum velocity occurred at 0.152 m/s on the tube side, which is depicted in Figure 7 (c). This indicates a decrease in the velocity of the working fluid because of the friction between the walls and the ZnO nanofluids. Consequently, there is a decrease in the centre line velocity of the fluid and

thus there is an enhancement of the heat transfer because of the increase in the retention time of the working fluid.

Case 2: Simulation of HCHE

The distribution of hot and cold fluid through the helical coil HE with a 2% ZnO mixture is represented in Figure 8 (a-c). The pressure distribution in the heat exchanger generated extreme pressure at 407 Pa and 7.483 Pa at the tube and shell sides, as depicted in Figure 8(a). similarly, maximum value of 352.9 K was observed in the distribution of temperature in the HE, as portrayed in Figure 7(b); therefore, it is evident from Figure 8(b) that the temperature on the tube side is reduced from 352.9 K to 304.35

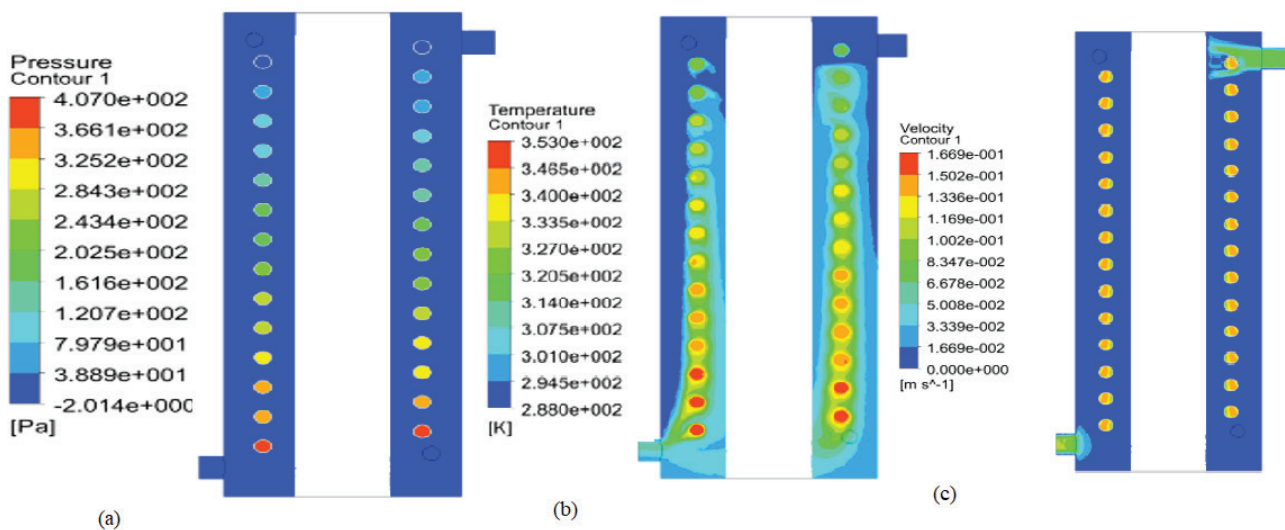


Figure 8. Contours of 2% ZnO as a cold side fluid for a mass flow rate of 0.175 kg/s.

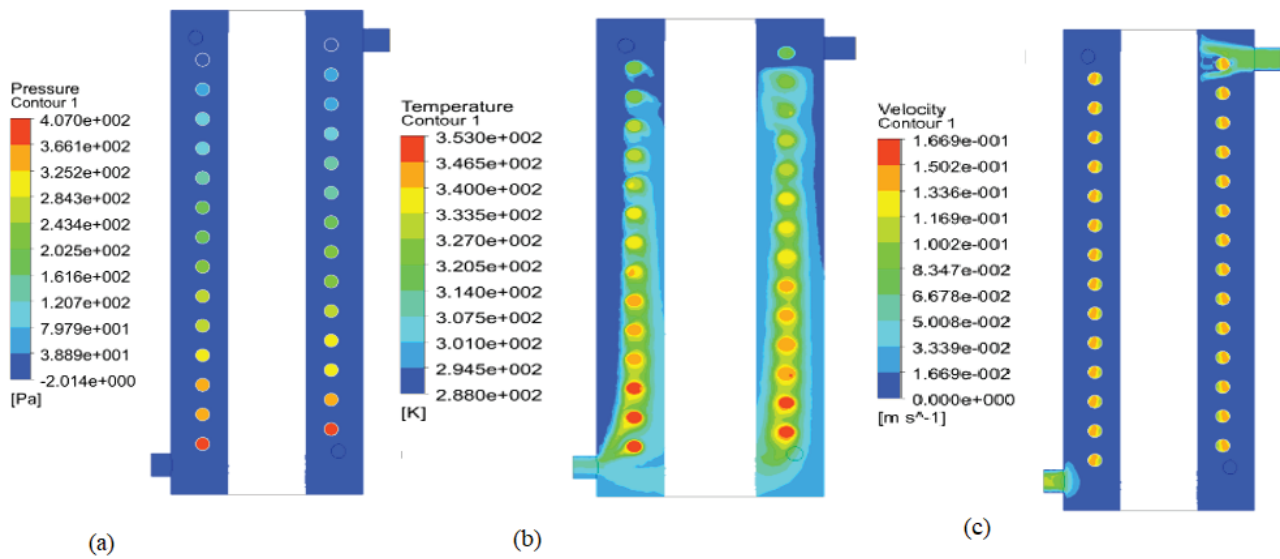


Figure 9. (a-c) Contours of 3% ZnO as a cold side fluid for a mass flow rate of 0.175 kg/s.

K with a decrement of 13.75%, this change is due to the existence of the heat (Q) transmission between hot as well as the cold fluids. The reason for this is again attributed to the increase in the concentration of the nanofluid, which increased the base fluid's thermal conductivity. Further, the Brownian motion of the nanofluid resulted in proper mixing of the nanoparticles with the base fluid and resulted in the enhancement of the heat transfer coefficient and thus in the enhancement of Nusselt number. The distribution of the velocity of the heat exchanger is represented in Figure 8(c) and resembles the maximum velocity occurrence of 0.419 m/s at the tube side. This depicts that the velocity is further reduced because of the wall friction and internal friction between the nanoparticles in the base fluid.

Case 3: Simulation of HCHE for ZnO with Volume Fraction of 3% and $\dot{m}=0.075$ kg/s

The distribution of hot and cold fluid through the helical coil HE with a 3% ZnO mixture is depicted in Figure 9 (a-c). The distribution of pressure in the heat exchanger is represented in Figure 9(a), which shows that the maximum pressure of 407 Pa and 23.03 Pa occurred at the tube and shell sides. This depicts that even though there is an increase in the concentration, there is not much drop in the pressure in comparison with the enhancement in the heat transfer. Hence, there is not much penalty in terms of friction factor. Similarly, the temperature distribution in the HE is portrayed in Figure 9(b); therefore, from the simulation, the changes in the figure indicate that the maximum temperature occurring is 352.9 K. However, the recorded values from the simulation reported that the temperature on the tube side was reduced to 293.72 K from 353 K due to the heat transmission between hot and cold fluid. From this figure, it was observed that there is an enhancement of heat transfer of 39% than the base fluid. This is because of

the reduction in the temperature with the increase in the circulation of the ZnO nanofluids. On the other side, the velocity distribution of the heat exchanger is demonstrated in Figure 9(c), confirming that the maximum velocity at the tube side was recorded as 0.3948 m/s.

Figure 10 presents the variation in heat transmission coefficient with flow rate (\dot{m}) for water ZnO nanofluids of various concentrations, i.e., 1%, 2%, and 3%. It gives a clear idea about how the heat transmission coefficient rises with the increased concentration of ZnO nanofluids. The observation from Figure 10 resembles that at 3% concentration of ZnO, the heat transmission coefficient is 39% higher than that with the base fluid. These changes occurred because of the Brownian mixing of the ZnO, nanofluids with the base fluid and the rise in thermal conductivity (K) of the carrier fluid due to the addition of the ZnO, nanoparticles. In a similar approach, the variation of friction factor with the flow rate for H_2O , ZnO nanofluids of various concentrations at 1.0%, 2.0% and 3.0% are plotted in Figure 11. The observation from the figure confirmed that the friction factor was 1.12 times greater with a 3% concentration of ZnO than the carrier-fluid by virtue of the collision between the nanoparticles and the nanoparticles with the walls. This results in the pressure drop inside the tubes. The heat transfer coefficient and friction factor of TiO_2 nanofluid flowing in a double pipe heat exchanger with and without helical coil inserts were experimentally studied by Reddy and Rao [35]. Helical coil inserts increased heat transmission and friction factor by 13.85% and 10.69%, respectively, according to the trial results 0.02% of the base fluid's nanofluid. Abu-Hamdeh et al. [36] showed that the Nusselt number will rise by 64.7%, 59.9%, 73.5%, and 62% for the semi-circular, quadrant, circular, inner side, and annulus side, respectively, if the Reynolds number is doubled in a helically coiled DPHE with the above cross-sections. Additionally, it

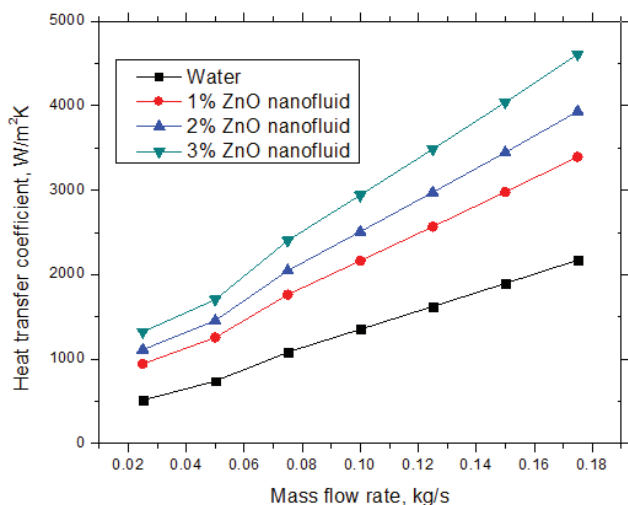


Figure 10. Variation of heat transfer coefficient with mass flow rate.

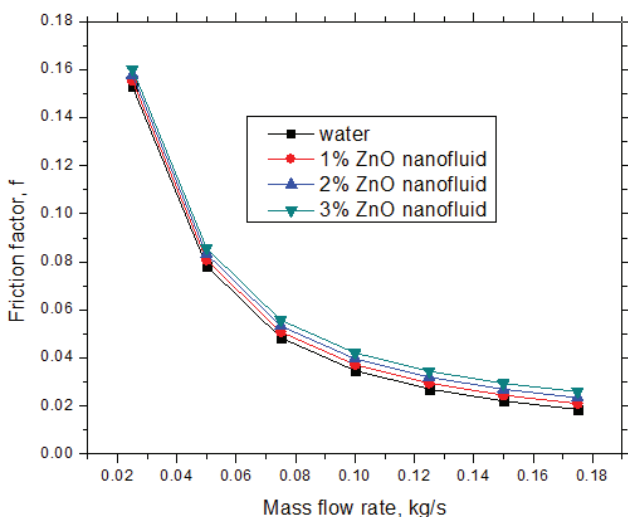


Figure 11. Variation of friction factor with mass flow rate.

was determined that a greater Reynolds number enhances the performance of the inner side, semi-circular, annulus side, and quadrant-circular cross-sections in that order.

CONCLUSION

Numerical simulation of a spiral tube heat exchanger is done with the heat transmission between shell to tube where the spiral tube is used to transport the cold fluid at a ‘m’ of 0.025 to 0.175 kg/s being considered for the nano-fluid homogenous mixture of 1% 2% and 3% respectively for zinc oxide and each of the cases is simulated with different volume fraction and all the masses from the results obtained with 3% volume concentration the heat transmission obtained is more compared to other cases compared for Nusselt number. The following conclusions are drawn:

1. The obtained results demonstrate that the heat transfer coefficient and friction factor enhanced by 39% and 1.12 times respectively using 3% concentration of ZnO nanofluid when compared with the plain tube.
2. The results indicate that the enhancement in the heat transfer is because of the helical shape of the coil, the increase in the thermal conductivity of the base fluid with the suspension of ZnO nanoparticles and the centrifugal forces that act on the fluid because of the helical coil in the heat exchanger.
3. The results also indicated that there is a less pressure drop which is offset by enhancement of heat transfer.

Finally, it can be concluded that the ZnO nanofluids can be used as heat transfer fluids in helical coil heat exchanger for better heat transfer.

NOMENCLATURE

kW	Kilowatt
USD/g	United States Dollar per gram
g/L	Gram per liter
CuO	Copper oxide
ZnO	Zinc oxide

ACKNOWLEDGMENT

The authors are thankful to the management of Raghu Engineering College for providing the necessary facilities for carrying out the analysis.

AUTHORSHIP CONTRIBUTIONS

Authors equally contributed to this work.

DATA AVAILABILITY STATEMENT

The authors confirm that the data that supports the findings of this study are available within the article. Raw data that support the finding of this study are available from the corresponding author, upon reasonable request.

CONFLICT OF INTEREST

The authors declared that they have no known conflicts of interest.

ETHICS

There are no ethical issues with the publication of this manuscript.

REFERENCES

- [1] Pulagam MKR. A state-of-the-art review on thermo fluid performance of brazed plate heat exchanger for HVAC application. J Therm Eng 2024;10:1390–1410. [CrossRef]

- [2] Pulagam MKR, Rout SK, Muduli KK, Syed SA, Barik D, Hussein AK. Internal finned heat exchangers: Thermal and hydraulic performance review. *Int J Heat Technol* 2024;42:583–592. [\[CrossRef\]](#)
- [3] Krishna Varma KPV, Venkateswarlu K, Nutakki UK, Satya Mohan KS. The effect of threaded rod inserts and aluminum oxide–water-based nanofluids on performance of a U-bend double pipe heat exchanger. *J Nanofluids* 2023;12:173–182. [\[CrossRef\]](#)
- [4] Burgles AE. *Handbook of Heat Transmission*. 3rd ed. New York: McGraw-Hill; 1998.
- [5] Burgles AE. The implications and challenges of enhanced heat transmission for the chemical process industries. *Chem Eng Res Des* 2001;79:437–444. [\[CrossRef\]](#)
- [6] Krishna Varma KPV, Kishore PS, Tulasi Tirupathi. CFD analysis for the enhancement of heat transmission in a heat exchanger with cut twisted tape inserts. *SSRG Int J Mech Eng* 2017;Special Issue: May.
- [7] Barai R, Kumar D, Wankhade A. Heat transfer performance of nanofluids in heat exchanger: a review. *J Therm Eng* 2023;9:86–106. [\[CrossRef\]](#)
- [8] Ali ARI, Salam B. A review on nanofluid: Preparation, stability, thermophysical properties, heat transfer characteristics and application. *SN Appl Sci* 2020;2:1636. [\[CrossRef\]](#)
- [9] Pattnaik PK, Syed SA, Mishra S, Jena S, Rout SK, Muduli K. Flow of viscous nanofluids across a non-linear stretching sheet. *J Therm Eng* 2023;9:593–601. [\[CrossRef\]](#)
- [10] Daungthongsuk W, Wongwises S. A critical review of convective heat transmission of nanofluids. *Renew Sustain Energy Rev* 2007;11:797–817. [\[CrossRef\]](#)
- [11] Jung JY, Oh HS, Kwak HY. Forced convective heat transmission of nanofluids in microchannels. *Int J Heat Mass Transf* 2009;52:466–472. [\[CrossRef\]](#)
- [12] Li Q, Xuan Y. Convective heat transmission and flow characteristics of Cu-water nanofluid. *Sci China Technol Sci* 2002;45:408–416. [\[CrossRef\]](#)
- [13] Eastman JA, Choi SUS, Li S, Yu W, Thompson LJ. Anomalous increase in effective thermal conductivities of ethylene glycol-based nanofluids containing copper nanoparticles. *Appl Phys Lett* 2001;78:718–720. [\[CrossRef\]](#)
- [14] Choi SUS, Zhang ZG, Yu W, Lockwood FE, Grulke EA. Anomalous thermal conductivity enhancement in nanotube suspensions. *Appl Phys Lett* 2001;79:2252–2254. [\[CrossRef\]](#)
- [15] Alami AH, Ramadan M, Tawalbeh M, Haridy S, Al Abdulla S, Aljaghoub H, et al. A critical insight on nanofluids for heat transmission enhancement. *Sci Rep* 2023;13:15303. [\[CrossRef\]](#)
- [16] Kola PVKV, Pisipaty SK, Mendu SS, Ghosh R. Optimization of performance parameters of a double pipe heat exchanger with cut twisted tapes using CFD and RSM. *Chem Eng Process* 2021;163:108362. [\[CrossRef\]](#)
- [17] Yang Y, Zhang ZG, Grulke EA, Anderson WB, Wu G. Heat transmission properties of nanoparticle-in-fluid dispersions (nanofluids) in laminar flow. *Int J Heat Mass Transf* 2005;48:1107–1116. [\[CrossRef\]](#)
- [18] Bahmani MH, Sheikhzadeh G, Zarringhalam M, Akbari OA, Alrashed AAAA, Shabani GAS, et al. Investigation of turbulent heat transmission and nanofluid flow in a double pipe heat exchanger. *Adv Powder Technol* 2018;29:273–282. [\[CrossRef\]](#)
- [19] Hasan FA. Numerical investigation of heat transmission rate in helically coiled pipe using Al₂O₃/water nanofluid. *Diyala J Eng Sci* 2020;13:27–36. [\[CrossRef\]](#)
- [20] Attia MEH, Hussein AK, Rout SK, Soli J, Elaloui E, Driss Z, et al. Experimental study of the effect of Al₂O₃ nanoparticles on the profitability of a single-slope solar still: Application in southeast Algeria. In: Ramgopal M, Rout SK, Sarangi SK, eds. *Advances in Air Conditioning and Refrigeration. Lecture Notes in Mechanical Engineering*. Singapore: Springer; 2021. pp. 119–133. [\[CrossRef\]](#)
- [21] Pulagam MKR, Rout SK, Sarangi SK. Numerical simulation of a brazed plate heat exchanger using Al₂O₃-water nanofluid with periodic boundary conditions. *WSEAS Trans Heat Mass Transf* 2023;18:262–270. [\[CrossRef\]](#)
- [22] Kola PVKV, Pisipaty SK, Mendu SS, Ghosh R. Optimisation of performance parameters of a double pipe heat exchanger with cut twisted tapes using CFD and RSM. *Chem Eng Process* 2021;163:108362. [\[CrossRef\]](#)
- [23] Palanisamy K, Mukesh Kumar PC. Experimental investigation on convective heat transmission and pressure drop of cone helically coiled tube heat exchanger using carbon nanotubes/water nanofluids. *Heliyon* 2019;5:e01705. [\[CrossRef\]](#)
- [24] Mukesh Kumar PC, Chandrasekar M. CFD analysis on heat and flow characteristics of double helically coiled tube heat exchanger handling MWCNT/water nanofluids. *Heliyon* 2019;5:e02030. [\[CrossRef\]](#)
- [25] Onyiriuka EJ, Ighodaro OO, Adelaja AO, Ewim DRE, Bhattacharyya S. A numerical investigation of the heat transmission characteristics of water-based mango bark nanofluid flowing in a double-pipe heat exchanger. *Heliyon* 2019;5:e02416. [\[CrossRef\]](#)
- [26] Gupta AK, Gupta B, Bhalavi J, Khandagre M. Enhancement of overall heat transmission coefficient of concentric tube heat exchanger using Al₂O₃/water nano-fluids. *JIRTI* 2019;4:41–46.
- [27] Arya H, Sarafraz MM, Pourmehran O, Arjomandi M. Heat transmission and pressure drop characteristics of MgO nanofluid in a double pipe heat exchanger. *Heat Mass Transf* 2019;55:1769–1781. [\[CrossRef\]](#)
- [28] Rafi S, Sivarajan DC, Mallikarjunch D. Optimisation of helical coil tube heat exchanger: A systematic review. *IOP Conf Ser Mater Sci Eng* 2020;998:012056. [\[CrossRef\]](#)

- [29] Kannadhasan V, Senthil Kumar A, Vairamuthu J, Nagarajan R. Experimental research and CFD analysis on double pipe heat exchanger with CuO nanoparticle suspended in cold water. *J Therm Anal Calorim* 2022;147:3831–3838. [\[CrossRef\]](#)
- [30] Inyang UE, Uwa IJ. Heat transmission in helical coil heat exchanger. *Adv Chem Eng Sci* 2022;12:26–39. [\[CrossRef\]](#)
- [31] Armstrong M, Mahadevan S, Selvapalam N, Santulli C, Palanisamy S, Fragassa C. Augmenting the double pipe heat exchanger efficiency using varied molar Ag ornamented graphene oxide (GO) nanoparticles aqueous hybrid nanofluids. *Front Mater* 2023;10:1240606. [\[CrossRef\]](#)
- [32] Nashine P, Singh TS. Effect of dean number on the heat transfer characteristics of a helical coil tube with variable velocity and pressure inlet. *J Therm Eng* 2020;6:128–139. [\[CrossRef\]](#)
- [33] Pesteei SM, Mashoofi N, Pourahmad S, Roshan A. Numerical investigation on the effect of a modified corrugated double tube heat exchanger on heat transmission enhancement and exergy losses. *Int J Heat Technol* 2017;35:243–248. [\[CrossRef\]](#)
- [34] Cengel YA, Ghajar AJ. *Heat and Mass Transfer: Fundamentals & Applications*. 4th ed. New York: McGraw-Hill; 2011.
- [35] Reddy MCS, Rao VV. Experimental investigation of heat transfer coefficient and friction factor of ethylene glycol water-based TiO₂ nanofluid in double pipe heat exchanger with and without helical coil inserts. *Int Commun Heat Mass Transf* 2014;50:68–76. [\[CrossRef\]](#)
- [36] Abu-Hamdeh NH, Bantan RAR, Tlili I. Analysis of the thermal and hydraulic performance of the sector-by-sector helically coiled tube heat exchangers as a new type of heat exchangers. *Int J Therm Sci* 2020;150:106229. [\[CrossRef\]](#)